

Synchronization in Gradient Networks

Xingang Wang,^{1,2} Ying-Cheng Lai,³ and Choy Heng Lai^{1,2}

¹*Department of Physics, National University of Singapore, 117542 Singapore*

²*Beijing-Hong Kong-Singapore Joint Centre for Nonlinear & Complex Systems (Singapore),
National University of Singapore, Kent Ridge, 119260 Singapore*

³*Department of Electrical Engineering,*

Department of Physics and Astronomy,

Arizona State University, Tempe, Arizona 85287, USA

(Dated: May 25, 2019)

Abstract

The contradiction between the fact that many empirical networks possess power-law degree distribution and the finding that network of heterogeneous degree distribution is difficult to synchronize has been a paradox in the study of network synchronization. Surprisingly, we find that this paradox can be well fixed when proper gradients are introduced to the network links, i.e. heterogeneity is in favor of synchronization in gradient networks. We analyze the statistical properties of gradient networks and explore their dependence to the other network parameters. Based on these understandings, we further propose a new scheme for network synchronization distinguished by using less network information while reaching stronger synchronizability, as supported by analytical estimates of eigenvalues and directed simulations of coupled chaotic oscillators. Our findings suggest that, with gradient, scale-free network is a natural choice for synchronization.

PACS numbers: 89.75.-k, 89.20.Hh, 05.10.-a

The study of complex networks has attracted a great deal of interest since the discoveries of the small-world [1] and scale-free [2] properties in many natural and man-made networks [3, 4, 5]. While in initial studies the nodes and links of a network are treated as identical, recent studies have extended to the heterogeneous networks of scaled nodes [6] and weighted links [7] where many new features and properties are discovered. Meanwhile, in many practical systems the scalars, which usually reflect the different characteristics among nodes, and the weights, which usually characterize the information transport capacities along links, are closely correlated. Typical examples include the co-authorship networks [8], where the scalar is the number of papers published by one researcher and the weight represents the collaboration times between two researchers, and the world-wide airline network [9], where the scalar can be the airport capacity and the weight denotes the amount of transportation between two airports. In both cases the links which connect nodes of larger scalar often assume higher weights. However, the latter is different to the former in that the transportation is directed and in most cases the mass flows in the two directions are not balanced, i.e., there exists *gradient* on the links. The gradient networks, which are defined as the directed graphs formed by local gradients of a scalar field distributed on the nodes, are ubiquitous in nature and have been shown to possess unique topology structures which could play an important role in biological and information transport processes [10, 11]. For example, in traffic networks of random scalar distributions, it is found that all non-degenerate gradient networks are forests, i.e. having no loops and consist only of trees, and the in-degree distributions follow a power-law scaling, regardless of whether the substrate networks are random or scale-free. It is also shown that the congestion tendency of traffic networks can be drastically reduced by gradient [10, 11].

It is well known that the collective behavior of complex systems is strongly influenced by their underling coupling structures. One challenging problem in this study which has arose continuous interest is chaos synchronization in complex networks [5, 12, 13]. Compare to the regular networks, the synchronizability of both the small-world and the scale-free networks (SFN) are drastically enhanced due to the decreased average distance [14], but, as shown by the recent studies [15, 16, 17], this propensity is effected by other network properties, e.g., the heterogeneous distributions of both the node degree and the link weight will suppress synchronizability. The contradiction between the fact that many empirical networks are heterogeneous and the finding that synchronizability are suppressed by heterogeneity has stimulated the investigations of how to construct optimal SFN for synchronization, this arises the question of how to distribute the coupling strength and set the coupling direction properly for a given system, which in turn led to the

study of weighted and directed networks [18, 19, 20, 21]. For weighted networks, in Ref. [18] the authors proposed to distribute the incoming coupling strengths according to the local information of node degree (hereafter we mark it as M-scheme). It is found that the synchronizability is solely determined by the average degree, independent of the degree distribution and the system size. In particular, under the condition of uniform coupling capacity, SFN achieves its maximum synchronizability which is superior to the homogeneous one. In Ref. [20] the incoming coupling strengths are proposed to be distributed according to the betweenness centrality of links (hereafter we mark it as C-scheme), it is found that synchronizability reaches its maximum only when the distributions of these two quantities match each other. In both cases, the couplings are directed and in general they are not balanced, i.e., one direction weights over another direction. Therefore the asymmetrically coupled network can be regarded as a superposition of two subgraphs: *one undirected symmetric network plus one directed gradient network*. While the former has been extensively studied and well recognized, this separation simplify the picture and make the gradient network distinct, now our attention solely turns to the study of gradient network and investigate its effects on network synchronization.

As more and more evidences point to the importance of gradient on synchronizability, an interesting question is: *which kind of gradient will maximize the synchronizability?* The answer relies on two parallel investigations: how to set the gradient direction and how to distribute the gradient weight. In setting the gradient direction, an intuitive method is to let the gradient start from the higher degree node and point to the lower one [18, 19, 20]. But analysis of non-diagonalizable networks suggest that this direction could be arbitrary given no loops in the gradient network [21]. In distributing the gradient weight, the answer is much diverse and confusing, the proposed methods range from the uniform weight distribution [19] (hereafter we marked it as H-scheme) to distributions based on local information of node degree [18, 21] and on global information of link betweenness [20]. An intriguing study is to compare the performance among all these schemes and find out the underlying mechanisms accounting for synchronizability enhancement.

In this paper, we will combine the works on gradient networks and chaos synchronization and build an unified framework for synchronization of asymmetric networks. We will first present the method of constructing gradient networks, analyze their statistical properties, and investigate the breaking problem when network parameters change. After this, we will propose a new coupling scheme for synchronization and, based on the method of eigenvalue analysis, compared its performance with the other schemes. We will also explain the diverse criteria in network synchronization

under the unified framework and identify the principles for constructing optimal networks. Finally, we will check our findings by direct numerical simulations on coupled chaotic oscillators.

We start by constructing the gradient network and analyze its topology structure. Since most empirical networks are scale-free, having a power-law distribution of node degree $P(k) \sim k^{-\gamma}$, and gradient networks, no matter the substrate is homogeneous random network (RN) or SFN, always possess the similar topology [10], here we choose SFN as the substrate to generate gradient network. For a SFN of N nodes and average degree $\langle K \rangle$ generated via the BA model [2], we associate with each node i a non-degenerate scalar, h_i , which is defined to be proportional to the node degree [18, 19]. *The gradient network is constructed as the collection of directed links pointing to each node from whichever of its near neighbors has the higher scalar.* If the neighbors have the same scalar or if the node has the same scalar as all its neighbors, the starting node will be randomly selected. Therefore the formed gradient network consists of N nodes and $\langle K \rangle \times N$ directed links. It can be proofed, following the similar formula in Ref. [10], that the gradient network is of tree structure and the out-degree follows a power-law distribution, $P(k) \sim k^{-\varsigma}$, with ς slightly smaller than 3 for scale-free substrate and $\varsigma \approx 1$ for random network of homogeneous degree distribution. These scalings are verified by numerical simulations, as plotted in Fig. 1(a).

While gradient from 'hubs' to 'nonhubs' has been identified as one of the main ingredients maximizing synchronizability [19], the network may suffer from the *risk* of breaking as gradient increases. To explain this, let's consider the extreme case where gradient takes over all the weights of a link [21], i.e. the symmetric network vanishes and only the gradient network keeps. If the 'hubs', which own high scalars and output gradient to their neighbors, are not directly linked, then each 'hub' will generate its own subsidiary graph. According to the construction rule of gradient network, these sub-graphs will be disconnected. As a result, the original network is separated into disconnected communities leading by each 'hub'. The chance for the network to break down is determined by two factors: the degree of heterogeneity and the average degree. *Homogeneous networks are easier to be broken than heterogeneous ones and, under the same degree of heterogeneity, sparse networks are easier to be broken than dense networks.* This is verified by numerical simulations as plotted in Fig. 1(b).

Despite of its negative effect on network breaking, gradient has been proofed to be an efficient method in tuning the collective behaviors of complex systems. For example, for coupled oscillators on lattice it has been shown that the increase of gradient could greatly enhance the synchronizability of the system [22]. The asymmetric coupling schemes proposed in Refs. [18, 19, 20] suggest

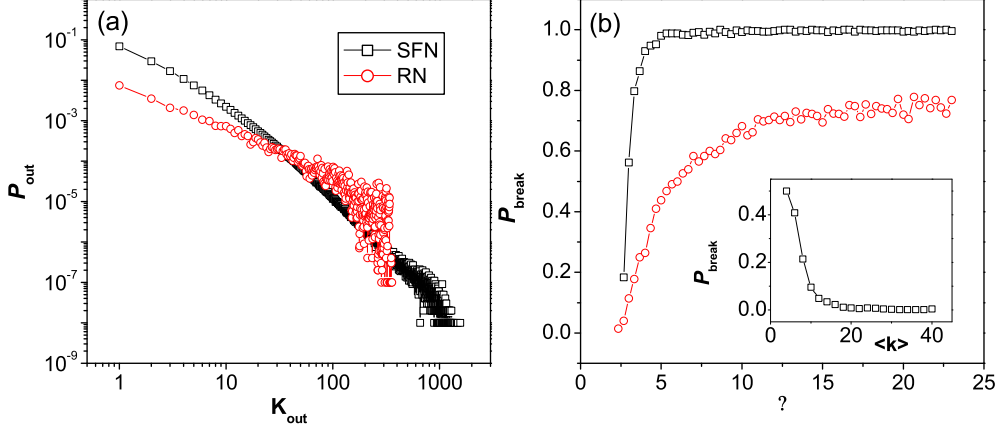


FIG. 1: For network of $N = 2^{10}$ nodes and mean degree $\langle k \rangle \geq 6$. (a) The out-degree distribution of gradient networks generated on SFN and RN substrates. Both distributions follow the power-law scaling with $\gamma \approx 2.8$ for SFN and $\gamma \approx 1$ for RN. (b) The probability of network breaking as a function of heterogeneity γ . Inset plots the breaking probability as a function of the mean degree $\langle k \rangle$. It is found that network tends to be breaking as γ increases or $\langle k \rangle$ decreases. Each data is an average result over 100 realizations.

this function applies to complex networks as well. The power of gradient is also shown in turbulence control, where the introduction of gradient could significantly improve the control efficiency [23]. Therefore, to improve the synchronizability, we need to set the gradient in a smart way. Based on the recent findings that 'hubs' are firstly synchronized than 'nonhubs' and performing as the core of pattern formation [24, 25], it is plausible to build *efficient* links between 'hubs' in the first place. Meanwhile, to guarantee that the synchronous manifold formed by the 'hubs' can be efficiently propagated to the 'nonhubs' while keeping its stability [19], then it is reasonable to put gradient from 'hubs' to 'nonhubs' with gradient weight proportional to the scalar difference. Finally, considering the fact that in most practical systems nodes are mutually coupled and the coupling capacity of node is limited, the gradient should be *adjustable* in weight.

Based on the above understandings, we go on to propose a new scheme for network synchronization. We consider networks of coupled chaotic oscillators following equations

$$\dot{\mathbf{x}}_i = \mathbf{F}(\mathbf{x}_i) - \varepsilon \sum_{j=1}^N G_{i,j} \mathbf{H}[\mathbf{x}_j], \quad i = 1, \dots, N, \quad (1)$$

where $\mathbf{F}(\mathbf{x}_i)$ governs the local dynamics of uncoupled node i , $\mathbf{H}[\mathbf{x}]$ is a linear coupling function and ε is the coupling strength. $G_{i,j}$ is a zero rowsum coupling matrix with off diagonal entries

read

$$G_{i,j} = \frac{L_{i,j}k_j^\beta}{\sum_{j=1}^N L_{i,j}k_j^\beta}, \quad i, j = 1, \dots, N, \quad (2)$$

with L the unweighted adjacency matrix of the underlying network: $L_{i,j} = -1$ if node i and node j is connected and $L_{i,j} = 0$ otherwise, k_j denotes the degree of node j , and β is a tunable parameter for gradient weight. The diagonal entries are unit $G_{i,i} = 1$.

We now compare the performance of the new proposed scheme with the former schemes which also employ asymmetric couplings [18, 19, 20]. The synchronizability of coupled networks can be evaluated by the method of master stability function (MSF) [27, 28], if the eigenvalues are reals, or by the method of eigenvalue analysis [22], if the eigenvalues are complex values. These methods tell us that the problem of synchronizability can be divided into two separating issues: the stability of the single dynamics $\mathbf{F}(\mathbf{x})$ and the distribution of eigenvalues of the coupling matrix G . For most systems, the single dynamics is stable within a certain range in the parameter space, $\sigma \in [\sigma_1, \sigma_2]$. The network is synchronizable iff all the eigenvalues except the one $\lambda_1 = 0$, which corresponding to the synchronous manifold, can be contained within this range after a linear scaling, i.e. $\lambda_N/\lambda_2 \leq \varepsilon\sigma_2/\sigma_1$, with λ_N the largest and λ_2 the smallest positive eigenvalues, respectively. In other words, the quantity of synchronizability can be described by eigenratio $R = \lambda_N/\lambda_2$, with a smaller R represents a higher synchronizability. Meanwhile, when network is synchronized, smaller λ_2 usually means lower coupling cost since $\lambda_2 > \sigma_1/\varepsilon$.

The eigenvalues of asymmetric matrix G are usually complex values [19, 22], but for coupling matrix of Eq. 2, they are reals. Noticing that the coupling matrix can be written as $G = QLD^\beta$, with $D = \text{diag}\{k_1, k_2, \dots, k_N\}$ the diagonal matrix of degrees and $Q = \text{diag}\{1/\sum_j L_{1,j}k_j^\beta, \dots, 1/\sum_j L_{N,j}k_j^\beta\}$ the normalization factors for rows of G . From the identity $\det(QLD^\beta - \lambda I) = \det(Q^{1/2}D^{\beta/2}LD^{\beta/2}Q^{1/2} - \lambda I)$ we find that the eigenvalues of the asymmetric matrix G are the same as that obtained from the symmetric matrix $H = Q^{1/2}D^{\beta/2}LD^{\beta/2}Q^{1/2}$, which are real and nonnegative values.

We go on to compare the effect of gradient among the different coupling schemes. In M-scheme the gradient is generated according to the degree difference and adjusted via parameter β_M , a negative value of β_M represents that the gradient flows from lower degree node to higher degree node, while for positive β_M the gradient flows in the opposite direction. As reported In Ref. [18] and replotted in Fig. 2(a), the maximum synchronizability happens at $\beta_M \approx 1$. Since the gradient increases its weight as β_M increases from 0, it is of certain surprise to find that, instead

of enhancement, larger gradients suppress synchronizability when $\beta_M > 1$. Another intriguing observation is the sharp change of eigenratio R as β varies: $R \approx 2 \times 10^3$ at $\beta_M = -1$ while $R \approx 6$ at $\beta_M = 1$. While the optimization at $\beta_M \approx 1$ can be understood by the heterogeneous distribution of the coupling capacity and the decreased coupling cost as β_M increases, the latter demonstrates the nontrivial effect of gradient played on network synchronization. In Fig. 2(a) we also plotted the variations of eigenratio as a function of the gradient degrees for C-scheme, where gradient is generated by the betweenness difference between the connected nodes, and for H-scheme, where gradient is generated by the aging difference. In the former scheme the weight of gradient is adjusted by parameter β_C , with negative values represent that the gradient flows from node of lower betweenness to node of higher betweenness, while the opposite happens for positive β_C . Again, the absolute value of β_C represents the weight of gradient. The behavior of R is quite similar to that of M-scheme, i.e. optimal configuration exists at around $\beta_C \approx 1$ while larger gradients suppress synchronizability, except that the variation of eigenratio is much smoother than that of M-scheme. For H-scheme the weight of gradient is adjusted via the parameter β_H , with negative values represent that the gradient flows from the 'older' node to the 'younger' node, while opposite happens for positive β_H . The absolute value of β_H represents the weight of gradient. Different to the former two schemes, it is found in Fig. 2(a) that for H-scheme the eigenratio R monotonically decreases as β_H decreases from 1 to -1 , or, similarly, as the gradient from 'older' to 'younger' increases its weight. Noticing that $\beta_H = 0$ equals the situation $\beta_M = 1$ in M-scheme, it seems that for H-scheme the increase of gradient will always enhance synchronizability. But the gradient network formed by this scheme is not of tree structure, which may delay the information propagation [21]. Meanwhile, a 'younger' node receives gradients *equally* from all its 'older' neighbors despite their detail difference, this may confuse the target synchronous state to which the 'younger' node should follow [15]. Therefore we predict that the function of gradient is not fully exploited in H-scheme.

As a comparison, we also plot in Fig. 2(a) the result of the new scheme described by Eq. 2. For $\beta < 0$, the gradient flows from lower degree node to higher degree node and the opposite happens when $\beta > 0$. The weight of gradient is adjusted by the absolute value of β . It can be found that, as β increases, the eigenratio R *monotonically* decreases from large values to small values. As we will show later, the smallest value that R can reach is only determined by the largest eigenvalue λ_N , which is almost constant for different coupling schemes. When $\beta = 0$, we recover the situations of $\beta_H = \beta_C = 0$ and $\beta_M = 1$ in the other schemes, respectively. Significantly, the

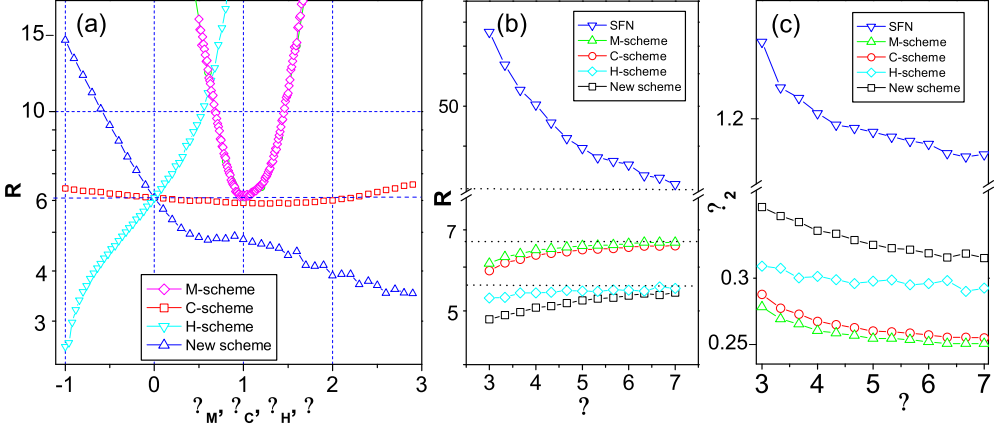


FIG. 2: For the same SFNs as in Fig. 1. (a) The variations of eigenratio R as functions of gradient weight β for different coupling schemes. (b) The eigenratio R as a function of degree heterogeneity γ for different schemes. The three dashed lines represent the eigenratio of RN under the situation of, from top to bottom, without gradient, with M-scheme, and with the new scheme of Eq. 2, respectively. (c) The variation of the λ_2 as a function of heterogeneity for different schemes. Each data is averaged over 50 realizations.

maximum synchronizability at $\beta_H = -1$ can be achieved at around $\beta \approx 5$, while R can be further decreased as β increases. In this sense, we say that the new scheme is more efficient in using the gradient than the other schemes.

Noticing the fact that increase of degree heterogeneity will suppress synchronizability [15], we go on to compare the synchronizabilities of the different schemes as a function of heterogeneity. The results are plotted in Fig. 2(b) together with three reference configurations: SFN without gradient, RN of M-scheme coupling, and RN of the new coupling scheme. To make the comparison fair, we adopt $\beta_M = 1$ and $\beta_C = 1$, where the maximum synchronizabilities are reached for the corresponding schemes. To make a fair comparison between the new scheme and the H-scheme, we adopt $\beta_H = -0.5$ and $\beta = 1.5$, since under this setting the total weight of gradient is equal for these two schemes. It can be found that the new scheme has a clear advantage over all the other schemes. It is also found that, under the new scheme, networks of higher heterogeneity shows a much clear advantage over the homogeneous ones, while for the other schemes the advantage is relatively weak. Therefore, we say that the new scheme not only efficiently enhances the synchronizability of SFNs, as compared with the original ones without gradient, but also makes them prominently superior to RN under the same coupling scheme. This may provide a more stronger explanation to the paradox found in network synchronization [18].

Another quantity used to characterize synchronizability is λ_2 , the second smallest eigenvalue. This is partially because some single dynamics $\mathbf{F}(\mathbf{x}_i)$ owns an open stable region in the coupling space [22], $\sigma \in [\sigma_1, \infty]$, and partially due to the finding that the change of λ_N is negligible when heterogeneity varies. The variation of λ_2 as a function of heterogeneity is plotted in Fig. 2(c), again, the new scheme shows a clear advantage over the other schemes.

To explore the underlying mechanisms behind the new scheme, we go on to characterize the gradient network by other two quantities: the distribution of gradient weight and the distribution of eigenvalues of coupling matrix G . The gradient weight is defined as $\Delta G_{i,j} = |G_{i,j} - G_{j,i}|$. In Fig. 3(a) we plot the weight distributions of the gradient networks for all the coupling schemes. A clear difference is that the weight distribution of the new scheme has a long tail. According to Eq. 2, a larger $\Delta G_{i,j}$ represents a larger degree difference between the connected nodes. This is in accordance with the second principle of network construction, i.e. the gradient weight should be proportional to the the degree difference. In contrary, in other schemes the node receives gradients from it neighbors relatively in a mean fashion. For example, In H-scheme, the 'younger' node receives equal gradient from all the 'older' neighbors, while disregards the difference among the neighbors. The advantage of the new scheme is also reflected in the distribution of eigenvalues. In Fig. 3(b) we plot the eigenvalue distributions for the different coupling schemes. It can be found that, while the largest eigenvalue λ_N is similar for all the schemes, the new scheme is distinct with a larger value of λ_2 and an absolutely higher probability around $\lambda = 1$. These properties make the eigenvalues restrict to a tight region around $\lambda = 1$, and directly deduce the value of eigenratio R . The extreme situation will be that all eigenvalues, except λ_N and λ_1 , equal 1, where the maximum synchronizability is achieved and $R = \lambda_N$.

From Figs. 3(a) and (b), it seems that increasing gradient will monotonically increases synchronizability. However, as shown in Fig. 1(b), too large gradients may suppress synchronizability instead, since stronger gradient brings higher probability of network breaking. Now we show these restrictions via eigenvalue analysis. In Fig. 3(c) we plot eigenratio R versus gradient degree β for networks of different heterogeneities. It is found that, as the heterogeneity increases, the large gradients gradually changes its role from enhancing synchronizability to suppress it. That is, for networks of lower heterogeneity and smaller mean degree, there exist an optimal gradient configuration at β_o . When $\beta < \beta_o$, increasing gradient will enhance synchronizability, but when $\beta > \beta_o$, the opposite happens. The network breaking at large gradient can be further understood by Fig. 3(d), where we plot the eigenratio R for a number of network realizations under the same

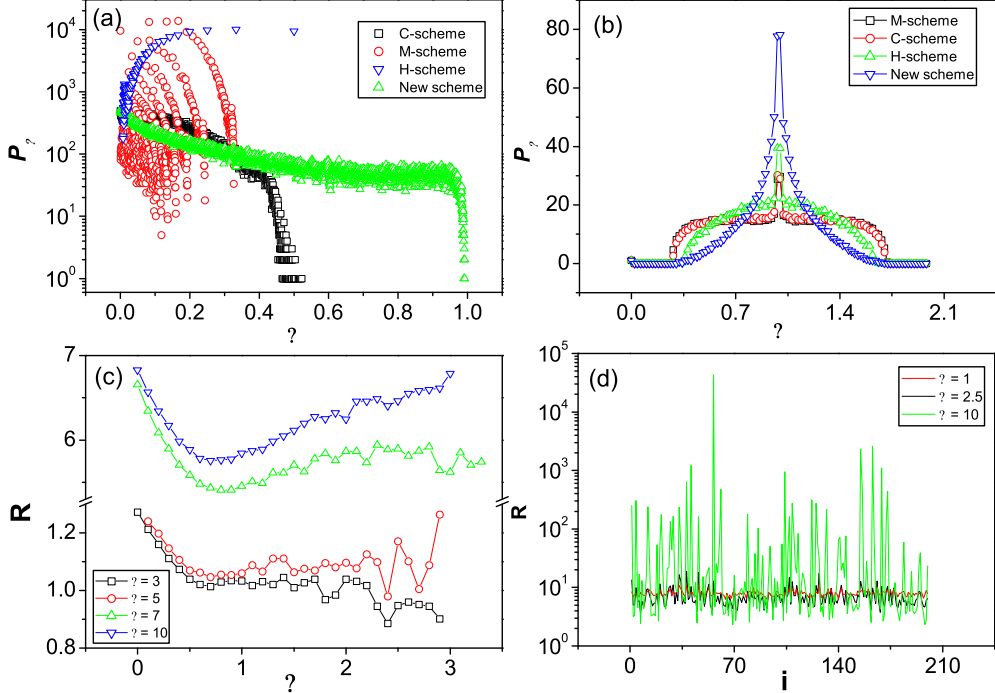


FIG. 3: For the same SFN as in Fig. 1. Comparing the distributions of gradient weight ΔG (a) and distributions of eigenvalues (b) among the different coupling schemes. (c) For the new scheme, the variation of R as a function of β for networks of different heterogeneities. Optimal gradient happens around $\beta_o \approx 0.7$ (d) The distribution of R as a function of sampling times for different β when $\gamma = 7$ in (c).

parameter set. It is found that, for networks of higher heterogeneity, the variance of R is small, representing a well connected network; but for networks of lower heterogeneity, R intermittently jumps to very large values, reflecting the breaking of networks at these points.

Finally, we provide the results of direct simulations. It was shown that, although the MSF method was proposed for complete synchronization of coupled identical systems, the eigenratio R could still provide a qualitative description for the collective behaviors, e.g. phase synchronization, of coupled nonidentical systems [18, 20, 24]. We employ SFN of nonidentical chaotic Rössler oscillators as the model. The dynamics of singular oscillator reads $\mathbf{F}_i(\mathbf{x}_i) = [-\omega_i y_i - z_i, \omega_i x_i + 0.15 y_i, z_i(x_i - 8.5) + 0.4]$, with ω_i the natural frequency of oscillator i , which is randomly assigned in range $[0.9, 1.1]$. The coupling form is $\mathbf{H}(\mathbf{x}) = \mathbf{x}$. The degree of synchronization in this model can be characterized by monitoring the amplitude A of the mean field $X = \sum_{i=1}^N x_i/N$ [18, 24]. For small coupling strength, X oscillates irregularly and A is approximately zero, reflecting a lower degree of synchronization; while X oscillates regularly and A increases sharply as coupling

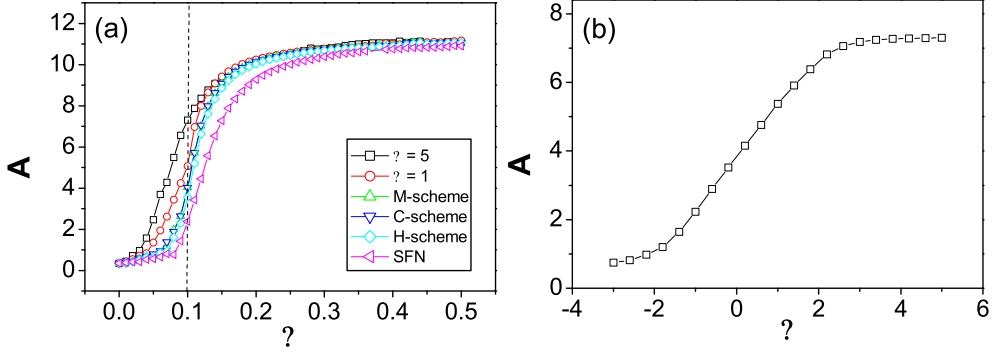


FIG. 4: For SFNs of $N = 2^{10}$ nodes and mean degree $\langle k \rangle \geq 10$, directed simulation of coupled non-identical Rössler oscillators. (a) The mean field amplitudes as a function of coupling strength for different coupling schemes. The parameters are $\beta_M = 1$ for M-scheme, $\beta_C = 1$ for C-scheme, $\beta_H = -0.5$ for H-scheme, $\beta = 1.5$ and 5 for the new scheme. The total gradient in H-scheme equals that of the new scheme. (b) For the new scheme, fixing $\varepsilon = 0.1$ in (a), the variation of mean field amplitude as a function of gradient. Each data is averaged over 10 realizations.

strength exceeds a critical value, reflecting a higher degree of synchronization. In Fig. 4(a) we plot the behavior of A as a function of the coupling strength ε for all the coupling schemes, it is found that the new scheme has a clear advantage over the other schemes even for smaller β , especially for the small ε region. To demonstrate the positive effect that gradient plays in the new scheme, we plot in Fig. 4(b) the behavior of A as a function of the gradient degree β . Again, as predicted by the eigenvalue analysis, A increases monotonically as β increases.

Another advantage enjoyed by the new scheme is that it employs only the local information of network in constructing the coupling matrix. While constructions based on global network information, e.g. the betweenness centrality in C-scheme and the oriented tree in Ref. [21], are possible for small size networks, the constructions based on local information, e.g. the node degree in M-scheme and node age in H-scheme, could be more efficient in practical. We note that in the new scheme the information, based on which the gradients of a node is distributed, relies on the degree of its neighbors, instead of the node itself. This is one of the key reasons which make the new scheme much efficient.

In conclusion, we have connected the study of gradient network to the problem of network synchronization and shown the significant role played by gradient in constructing optimal complex networks. Under this framework, previous studies on asymmetric networks can be well unified and

the principles for synchronizability enhancement become simple and vivid. Our studies not only indicates, comparing to homogeneous networks, that scale-free networks are the natural choice for synchronization, but also predict that, for practical networks of low heterogeneity and small mean degree, there exists an optimal gradient degree at which the synchronizability is maximized. We expect this prediction to be verified by empirical findings in future.

YCL was supported by NSF under Grant No. ITR-0312131 and by AFOSR under Grant No. FA9550-06-1-0024.

- [1] D.J. Watts and S.H. Strogatz, *Nature* **393**, 440 (1998).
- [2] A.-L. Barabási and R. Albert, *Science* **286**, 509 (1999).
- [3] R. Albert and A.-L. Barabási, *Rev. Mod. Phys.* **74**, 47 (2002).
- [4] M.E.J. Newman, *SIAM Rev.* **45**, 167 (2003).
- [5] S. Boccaletti, V. Latora, Y. Moreno, M. Chavez, and D.-U. Hwang, *Phys. Rep.* **424**, 175 (2006).
- [6] G. Bianconi and A.-L. Barabási, *Europhys. Lett.* **54**, 436 (2001).
- [7] S.H. Yook, H. Jeong, A.-L. Barabási and Y. Tu, *Phys. Rev. Lett.* **86**, 5835 (2001).
- [8] M.E.J. Newman, *Proc. Natl. Acad. Sci. U.S.A.* **98**, 404 (2001).
- [9] R. Guimerá, S. Mossa, A. Turtschi, and L.A.N. Amaral, *Proc. Natl. Acad. Sci. U.S.A.* **102**, 7794 (2005)(wan).
- [10] Z. Toroczkai and K.E. Bassler, *Nature*, **428**, 716 (2004); Z. Toroczkai, B. Kozma, K.E. Bassler, N.W. Hengartner, and G. Korniss, e-print cond-mat/0408262.
- [11] K. Park, Y.-C. Lai, L. Zhao, and N. Ye, *Phys. Rev. E* **71**, 065105 (2005).
- [12] A.S. Pikovsky, M.G. Rosenblum, and J. Kurths, *Synchronization: A Universal Concept in Nonlinear Science* (Cambridge University Press, Cambridge, 2001).
- [13] S. Boccaletti and L.M. Pecora, *Chaos* **16**, 015101 (2006).
- [14] X.F. Wang and G. Chen, *Int. J. Bifurcation Chaos Appl. Sci. Eng.* **12**, 187 (2002).
- [15] T. Nishikawa, A.E. Motter, Y.-C. Lai, and F.C. Hoppensteadt, *Phys. Rev. Lett.* **91**, 014101 (2003).
- [16] M. Denker, M. Timme, M. Diesmann, F. Wolf, and T. Geisel, *Phys. Rev. Lett.* **92**, 074103 (2004).
- [17] C. Zhou, A.E. Motter, and J. Kurths, *Phys. Rev. Lett.* **96**, 034101 (2006).
- [18] A.E. Motter, C. Zhou, and J. Kurths, *Europhys. Lett.* **69**, 334 (2005); *Phys. Rev. E* **71**, 016116 (2005); AIP Conf. Proc. **776**, 201 (2005).

- [19] D.-U. Hwang, M. Chavez, A. Amann, and S. Boccaletti, Phys. Rev. Lett. **94**, 138701 (2005).
- [20] M. Chavez, D.-U. Hwang, A. Amann, H.G.E. Hentschel, and S. Boccaletti, Phys. Rev. Lett. **94**, 218701 (2005).
- [21] T. Nishikawa and A.E. Motter, Phys. Rev. E **73**, 065106 (2006).
- [22] J. Yang, G. Hu and J. Xiao, Phys. Rev. Lett. **80**, 496 (1998); G. Hu, J. Yang and W. Liu, Phys. Rev. E **58**, 4440 (1998).
- [23] J. Xiao, G. Hu, J. Yang, and J. Gao, Phys. Rev. Lett. **81**, 5552 (1998); G. Hu, J. Xiao, J. Gao, X. Li, Y. Yao and B. Hu, Phys. Rev. E **62**, 3043 (2000).
- [24] C. Zhou and J. Kurths, Chaos **16**, 015104 (2006).
- [25] P.N. McGraw and M. Menzinger, Phys. Rev. E **72**, 015101 (2005).
- [26] S.N. Dorogovtsev, J.F.F. Mendes, and A.N. Samukhin, Phys. Rev. Lett. **85**, 4633 (2000).
- [27] L.M. Pecora and T.L. Carroll, Phys. Rev. Lett. **80**, 2109 (1998).
- [28] M. Barahona and L.M. Pecora, Phys. Rev. Lett. **89**, 054101 (2002).